United States
Department of
Agriculture

Forest Service

Forest
Products
Laboratory

Madison
Wisconsin

Research
Paper
FPL 343

May 1979

Analysis of Orthotropic Beams

ABSTRACT

A plane-stress analysis of orthotropic or isotropic beams is presented. The loading conditions considered are: (1) a concentrated normal load arbitrarily located on the beam, and (2) a distributed normal load covering an arbitrary length of the beam. Other loading conditions can similarly be considered. Numerical results based on the present analysis exhibit close agreement with existing experimental data from Sitka spruce beams.

CONTENTS

ANALYSIS OF ORTHOTROPIC BEAMS

By

J. Y. LIU[1/]
and
S. CHENG[2/]

INTRODUCTION

The solution of the plane-stress or plane-strain problem for an infinite strip of orthotropic material was studied by Green (7).[3/] In his solution, both the upper and lower boundaries of the strip must be loaded, a situation not commonly encountered in engineering applications. Using a similar approach by Lamb (10) for a narrow beam of isotropic material, Smith and Voss (12) solved the problem of a beam of either isotropic or orthotropic material with a concentrated load applied at the center of the span. Conway (2) used polynomial stress functions in his solutions of an orthotropic cantilever beam loaded at the free end and a simply supported beam under uniformly distributed loads. He also solved the problem of a deep beam of orthotropic material symmetrically loaded with respect to the beam axis (3). Functions were derived by Silverman (11) to describe the stresses and displacements of orthotropic beams under distributed polynomial loads. Hashin (8) developed a method to solve the elasticity problem of long plane anisotropic rectangles with continuous polynomial stresses prescribed on the long sides, and force and moment resultants prescribed at the ends. The problems analyzed in (2,11) were discussed in detail for anisotropic material in (8). The finite element technique was applied by Hooley and Hibbert (9) to solve the plane-stress problem of a wood beam. This numerical technique, while applicable to intricate boundary conditions, is limited by the computer capacity; also, in areas of high stress concentrations where interpolation procedures must be followed for stress estimations, the method cannot yield accurate results.

1/ Engineer, Forest Products Laboratory, Forest Service, U.S. Dep. of Agric., Madison, Wis.

2/ Professor, Engineering Mechanics Department, University of Wisconsin, Madison, Wis.

3/ Numbers in parenthesis refer to references cited near end of report.

For narrow, rectangular beams of isotropic material, solutions for some specified loading and support conditions can be found in (13). Donnell (5) applied infinite series for stresses in his solution with the first terms corresponding to elementary theory and the latter terms to increasingly minor refinements. However, his solution cannot be applied where discontinuities exist, and the most serious such discontinuity is that caused by a concentrated load. Boley and Tolins (1) used an iterative procedure to analyze the two-dimensional beam problem. The applied loads considered by them may consist of either normal or shear forces varying smoothly along the span.

Experiments were performed by Cowan (4) to determine the horizontal shear stress distribution in beams of Sitka spruce. He found that in the vicinity of a bearing support, the shear stress distributions were considerably different from what the simple beam theory would predict. The same phenomenon was observed in (12) to exist in the vicinity of a load point.

In the study presented herein the practical loading conditions not discussed in the cited literature will be considered, namely: (1) a concentrated normal load arbitrarily located on the beam, and (2) a distributed normal load covering an arbitrary length of the beam. With these solutions available, a large number of practical beam problems can be handled using the method of superposition.

THEORETICAL ANALYSIS

The beam considered is assumed to be an orthotropic solid having its edges parallel to two perpendicular axes of elastic symmetry. The thickness of the beam is assumed small as compared with the vertical depth so that the problem can be treated as one of plane stress.

The x-axis is taken along the center line of the beam and the y-axis coincident with the left end of the beam as shown in figure 1(a).

For the isotropic case, the pertinent derivations are presented in Appendix I.

STRESS AND LOAD FUNCTIONS

For the state of plane stress in the orthotropic beam, the stress function, ϕ, must satisfy the following equation of compatibility (12):

$$\frac{\partial^4 \phi}{\partial x^4} + 2K \frac{\partial^4 \phi}{\partial x^2 \partial \eta^2} + \frac{\partial^4 \phi}{\partial \eta^4} = 0 \qquad (1)$$

where

$$K = \frac{\sqrt{E_x E_y}}{2} \left(\frac{1}{G_{xy}} - \frac{2\nu_{xy}}{E_x} \right) \qquad (1a)$$

$$\eta = \varepsilon y \qquad (1b)$$

$$\varepsilon = \sqrt[4]{\frac{E_x}{E_y}} \qquad (1c)$$

Equation 1 may be satisfied by taking the function ϕ in the form

$$\phi = \sum_{n=1}^{\infty} f(\eta) \sin \frac{n\pi x}{\ell} \qquad (2)$$

In which $f(\eta)$ is a function of η only. Substituting equation 2 into equation 1 and using the notation $m = n\pi/\ell$, one finds the following equation for determining $f(\eta)$:

$$m^4 f - 2Km^2 \frac{d^2 f}{d\eta^2} + \frac{d^4 f}{d\eta^4} = 0 \qquad (3)$$

The general integral of this linear differential equation with constant coefficients is

$$f(\eta) = A_n \cosh m\alpha\eta + B_n \cosh m\beta\eta + C_n \sinh m\alpha\eta + D_n \sinh m\beta\eta \qquad (4)$$

where

$$\alpha = \sqrt{K + \sqrt{K^2 - 1}} \tag{4a}$$

and

$$\beta = \sqrt{K - \sqrt{K^2 - 1}} \tag{4b}$$

The stress function is then obtained by substituting equation 4 into equation 2, and the corresponding stress components are

$$\sigma_x = \varepsilon^2 \frac{\partial^2 \phi}{\partial \eta^2} = \varepsilon^2 \sum_{n=1}^{\infty} m^2 (A_n \alpha^2 \cosh m\alpha\eta + B_n \beta^2 \cosh m\beta\eta + C_n \alpha^2 \sinh m\alpha\eta + D_n \beta^2 \sinh m\beta\eta) \cdot \sin mx \tag{5}$$

$$\sigma_y = \frac{\partial^2 \phi}{\partial x^2} = - \sum_{n=1}^{\infty} m^2 (A_n \cosh m\alpha\eta + B_n \cosh m\beta\eta + C_n \sinh m\alpha\eta + D_n \sinh m\beta\eta) \cdot \sin mx \tag{6}$$

$$\tau = -\varepsilon \frac{\partial^2 \phi}{\partial x \partial \eta} = -\varepsilon \sum_{n=1}^{\infty} m^2 (A_n \alpha \sinh m\alpha\eta + B_n \beta \sinh m\beta\eta + C_n \alpha \cosh m\alpha\eta + D_n \beta \cosh m\beta\eta) \cdot \cos mx \tag{7}$$

in which the constants A_n, B_n, C_n, and D_n are to be determined from the loading conditions and τ represents τ_{xy}.

Assuming that the load function can be expressed as a Fourier series,

$$p(x) = \sum_{n=1}^{\infty} a_n \sin \frac{n\pi x}{\ell} \tag{8}$$

the coefficients a_n in equation 8 can be written as

$$a_n = \frac{2}{\ell}\int_0^{\ell} p(x)\sin \frac{n\pi x}{\ell}\, dx \tag{8a}$$

Let p (x) be represented by $P/2\xi$ acting at x = a as shown in figure 1(b).

Then

$$a_n = \frac{2p}{\ell 2\xi}\int_{a-\xi}^{a+\xi} \sin \frac{n\pi x}{\ell} dx$$

$$= \frac{2p}{n\pi\xi} \sin \frac{n\pi a}{\ell} \sin \frac{n\pi\xi}{\ell} \tag{8b}$$

For a concentrated load P acting at x = a, one obtains from equation 8b

$$\lim_{\xi \to 0} a_n = \frac{2P}{\ell} \sin \frac{n\pi a}{\ell} \tag{8c}$$

Hence, for any specified loading condition, the load function can be expressed as a Fourier series following the above procedure to be consistent with the stress function defined by equation 2.

METHOD OF SOLUTION

To determine A_n, B_n, C_n, and D_n in equations 5, 6, and 7, four boundary conditions are needed. Consider the problem described in figure 1(b). The four boundary conditions are:

(1) $\sigma_y = p(x)$ at $y = h$ (9)

(2) $\tau = 0$ at $y = h$ (10)

(3) $\sigma_y = 0$ at $y = -h$ (11)

(4) $\tau = 0$ at $y = -h$ (12)

From these boundary conditions, one obtains

$$A_n = \frac{D_a}{D}\ ,\ B_n = \frac{D_b}{D}\ ,\ C_n = \frac{D_c}{D}\ ,\ D_n = \frac{D_d}{D} \tag{13}$$

where

$$D = m^2\left[1 - \tfrac{1}{2}(\alpha^2 + \beta^2)\right]\cosh 2m\alpha\cosh(\alpha+\beta)$$

$$+m^2\left[1 + \tfrac{1}{2}(\alpha^2 + \beta^2)\right]\cosh 2m\alpha\cosh(\alpha-\beta)$$

$$- 2m^2 \tag{13a}$$

$$D_a = \frac{a_n}{2}\left[(\beta^2-1)\cosh m\alpha\cosh(\alpha+2\beta)\right.$$

$$\left. - (\beta^2+1)\cosh m\alpha\cosh(\alpha-2\beta) + 2\cosh m\alpha\cosh\right] \tag{13b}$$

$$D_b = \frac{a_n}{2}\left[(\alpha^2-1)\cosh m\alpha\cosh(2\alpha+\beta)\right.$$

$$\left. - (\alpha^2+1)\cosh m\alpha\cosh(2\alpha-\beta) + 2\cosh m\beta\cosh\right] \tag{13c}$$

$$D_c = \frac{a_n}{2}[(\beta^2-1)\sinh m\varepsilon h(\alpha+2\beta) - (\beta^2+1)\sinh m\varepsilon h(\alpha-2\beta) - 2\sinh m\alpha\varepsilon h] \quad (13d)$$

$$D_d = \frac{a_n}{2}\{(\alpha^2-1)\sinh m\varepsilon h(2\alpha+\beta) + (\alpha^2+1)\sinh m\varepsilon h(2\alpha-\beta) - 2\sinh m\beta\varepsilon h] \quad (13e)$$

It is noted that equations 13 are applicable for a_n corresponding to any loadfunction. It is also noted that if the load were applied on the lower side of the beam, all that need be done is to change the sign for h in equations 9-12.

The infinite series obtained by substituting equation 13 into equations 5, 6, and 7 can easily be solved using a digital computer. In order to save on computer storage and time, a method of reducing the infinite series to the sum of a finite series and a closed form is described in Appendix II.

DEFLECTION OF BEAM

Deflection of a beam may indicate its performance under specified loadingconditions. It may also serve to derive the reactions in an indeterminate situation. From the strain-displacement relationships and the generalized Hooke's law, the following equations can be obtained:

$$E_x u = \int (\sigma_x - \nu_{xy}\sigma_y)dx + r(y) \quad (14)$$

$$E_y v = \int (\sigma_y - \nu_{yx}\sigma_x)dy + s(x) \quad (15)$$

where u and v are the displacements in the x- and y-directions, respectively. Also,

$$\frac{\tau}{G_{xy}} = \frac{\partial u}{\partial y} + \frac{\partial v}{\partial x} = \frac{1}{E_x}\left[\int \left(\frac{\partial \sigma_x}{\partial y} - \nu_{xy}\frac{\partial \sigma_y}{\partial y}\right)dx + \frac{dr}{dy}\right] + \frac{1}{E_y}\left[\int \left(\frac{\partial \sigma_y}{\partial x} - \nu_{yx}\frac{\partial \sigma_x}{\partial x}\right)dy + \frac{ds}{dx}\right] \quad (16)$$

From the stress expressions in equations 5, 6, and 7, it is evendent that in equation 16 the following relation must hold true

$$\frac{1}{E_x}\frac{dr}{dy} + \frac{1}{E_y}\frac{ds}{dx} = 0 \quad (17)$$

Let

$$\frac{1}{E_x}\frac{dr}{dy} = K_o$$

Then

$$r = E_x K_o y + K_1 \quad (18)$$

Likewise,

$$\frac{1}{E_y}\frac{ds}{dx} = -K_o$$

and

$$s = -E_y K_o x + K_2 \tag{19}$$

The constants K_o, K_1, and K_2 in equations 18 and 19 are to be determined from the known displacements at the supports.

Usually, only the vertical deflection of the beam center line is of interest in engineering applications. One then obtains from equations 5, 6, 15, and 19, the following expression

$$E_y v = -\sum_{n=1}^{\infty} m[C_n(\frac{1}{\varepsilon\alpha} + \nu_{yx}\varepsilon\alpha) + D_n(\frac{1}{\varepsilon\beta} + \nu_{yx}\varepsilon\beta)] \cdot \sin mx - E_y K_o x + K_2 \tag{20}$$

For a beam whose vertical displacements at the two ends are zero, it is seen that both K_o and K_2 in equation 20 must vanish.

NUMERICAL RESULTS

Numerical calculations were made for the wood beams used in Cowan's experiments (4) for shear stress measurements using a Univac 1100 computer. In his experiments, a simple beam and a two-span continuous beam were used, which were clear straight-grained specimens of Sitka spruce. Supports and load blocks also were of Sitka spruce to simulate actual constructionconditions.

For the simple beam, the applied load and reactions and the geometrical dimensions from (4) are shown in figure 2. The right support is a roller-type support, but the left support is a flat bearing block restrained against horizontal movement. Hence, the left support could be assumed to approximate a hinged support with resultant of the reaction forces acting closer to the load point. The reaction forces at the left support are therefore assumed to be distributed as shown in figure 2(b). The material properties taken from (4) were as follows:

$E_x = 1.84 \times 10^6$ psi $(1.2686 \times 10^{10}$ N/m$^2)$

$E_y = 6.62 \times 10^4$ psi $(4.5643 \times 10^8$ N/m$^2)$

$G_{xy} = 1.089 \times 10^5$ psi $(7.5083 \times 10^8$ N/m$^2)$

$\nu_{xy} = 0.26$

$\nu_{yx} = 0.0094$

Figure 3 presents the orthogonal shear stress distributions in the beam at the left support. The theoretical predictions and the experimental data are seen to agree closely with each other. The differences are, of course, due to the material heterogeneity and the assumed stress distribution at the support. It is to be noted that the stresses in the beam are strongly dependent on the stress distribution at the support which can only be estimated.

The vertical compressive stress distributions are shown in figure 4. By comparing figures 3(c) and 3(d) with figure 4, it is seen that the large shear stresses do not always occur where the vertical compressive stresses are high.

The bending stresses plotted in figure 5 are seen to be highly non-linear and are negative in both the upper and lower regions of the beam above the support.

Figure 6 shows the applied loads and reactions and the dimensions of the two-span continuous beam. The middle reaction is a flat bearing block of wood 8 inches long. However, due to material variabilities, the resultant of the reaction forces was found to be 2 inches on the right of the center of the middle support. In the numerical calculations, the reaction forces are then assumed to be distributed as described in figure6(b).

The material properties for this beam were the same as those for the simple beam except the modulus of rigidity was found to be 1.121×10^5 psi $(7.7289 \times 10^8$ N/m$^2)$ rather than 1.089×10^5 psi $(7.5083 \times 10^8$ N/m$^2)$ according to (4).

The shear stress distributions at the middle support are shown in figure7. Due to the material heterogeneity and the inherent experimental inexactness, considerable randomness exists in the experimental data. However, the variations of the experimental shear stress with location follow generally the same trend as predicted theoretically.

The vertical compressive stress distributions plotted in figure 8 disclose their strong dependency on the assumed reactive forces at the support. This is, of course, partly due to the relatively large distances of the applied loads and the end supports from the middle support.

At a given depth of the beam, the nonlinear bending stresses are seen to vary only slightly across the length of the support as described in figure 9.

Numerical calculations were also performed for the simple beam of Sitka spruce loaded at the center as reported in (12). For a concentrated central load, the theoretical predictions of the shear stresses in the vicinity of the load point of the present study and of reference (12) are essentially the same. In (12), the following function was used for a unit load acting on the beam:

$$\bar{\phi}(x) = \frac{\delta}{\pi} \frac{1}{x^2 + \delta^2} \qquad (21)$$

where x is measured from the center of an infinitely long beam along its axis and the value of δ is related to the length covered by the load. For $\delta = 0$, the load is concentrated; for small values of δ, equation 21 was assumed suitable for representation of a load applied over a small area by a curved loading block. In the test reported in (12), the central load was applied over a length of about 0.4 inch (10.16 mm) by a cylindrical block. At a point close to the load, the calculated shear for $\delta = 0$ inch (0 mm) was 235 psi (1.6202×10^6 N/m^2) and for $\delta = 0.25$ inch (6.35 mm) was 116 psi (7.9978×10^5 N/m^2), which was close to the measured value. Based on the present work, the calculated shear for $\xi = 0$ inch (0 mm) was 234 psi (1.6134×10^6 N/m^2), for $\xi = 0.2$ inch (5.08 mm) was 229 psi (1.5789×10^6 N/m^2) and for $\xi = 0.3$ inch (7.62 mm) was 212 psi (1.4617×10^6 N/m^2). To reduce the shear stress to the measured value, the length covered by the load must be much larger than 0.6 inch (15.24 mm). It is believed that the measured value at that point is likely to be in error and δ cannot be properly used to represent a load over a specified small length. In fact, the statement made in (12) that 84 percent of the area under the curve of equation 21 is over a length 2δ on either side of $x = 0$ is wrong. It can be shown that for a length of 2δ, the percentage is 50; for a length of 4δ, the percentage is 70; and for a length of 8δ, the percentage is 84.

For the isotropic case, the calculated stresses and deflections based on the present work agree with the best estimations in (13) for a simple beam loaded at the middle.

DISCUSSION AND CONCLUSION

The present analysis demonstrates a procedure for calculating the stresses and deflection of a two-dimensional orthotropic or isotropic beam under arbitrary loading conditions. In the solutions, each of the infinite series has been reduced to the sum of a finite series and a closedform, making it possible to obtain accurate numerical results using a computer of relatively small capacity.

Numerical results based on the present work indicate that they are in reasonable agreement with existing experimental data. For specified loading conditions that can be considered by existing theories, e.g., (12) and (13), the present method can yield the same predictions as the othertheories.

The method is very useful in predicting the stress distributions in a beam, especially in the vicinity of a support or a nominal load point. However, for the latter purpose, the reactive stresses at a support or the acting stresses at a nominal load point must be correctly estimated in order to obtain accurate results.

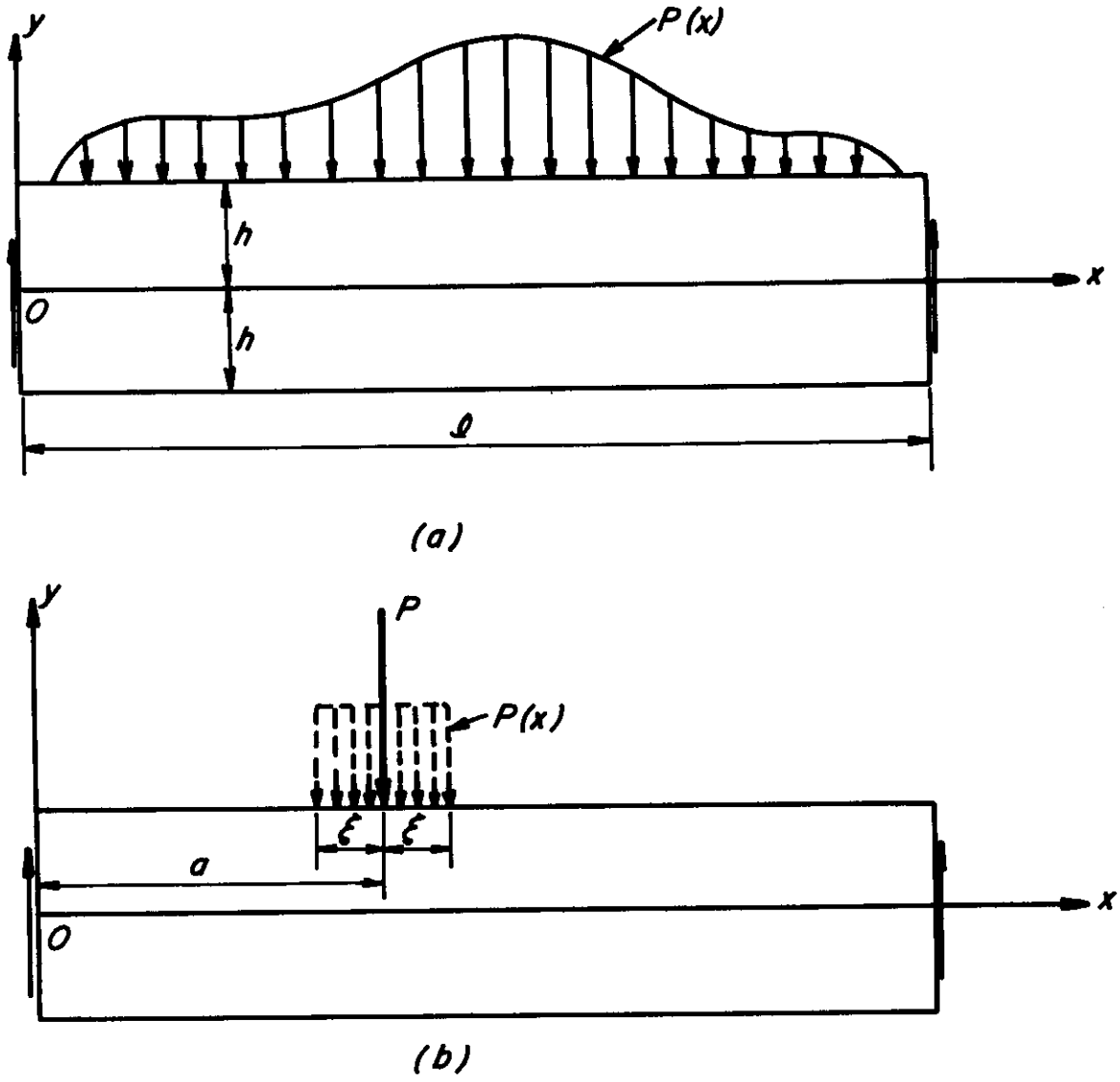

Figure 1.--(a) Coordinate system and geometry of beam

(b) load function and load location on beam.

(M 146 766)

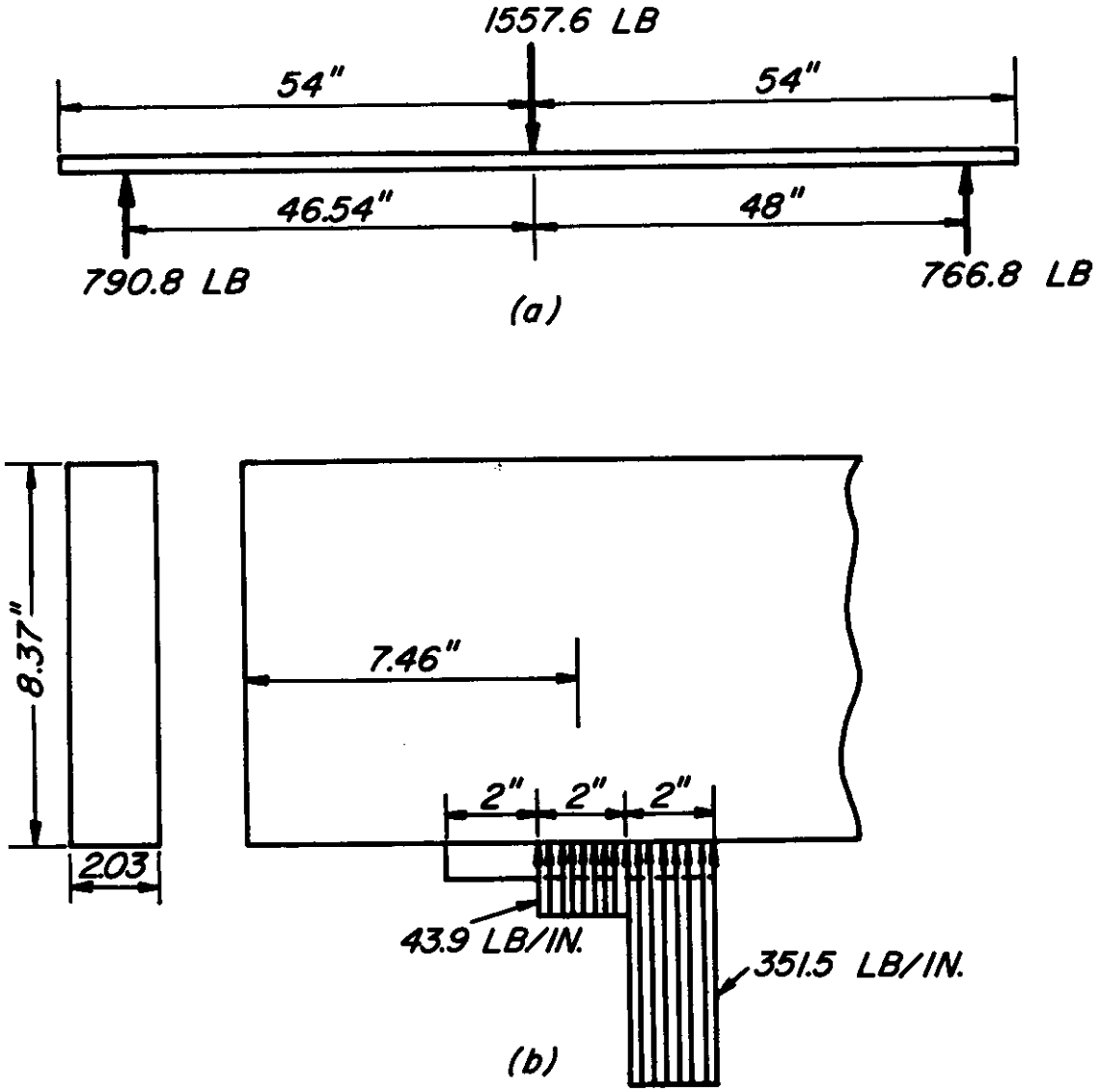

Figure 2.--Simple beam (a) applied load and reactions; (b) assumed compressive forces at left support (1 in. = 25.4 mm; 1 lb. = 4.4482 N; 1 lb./in. = 175 N/m).

(M 146 767)

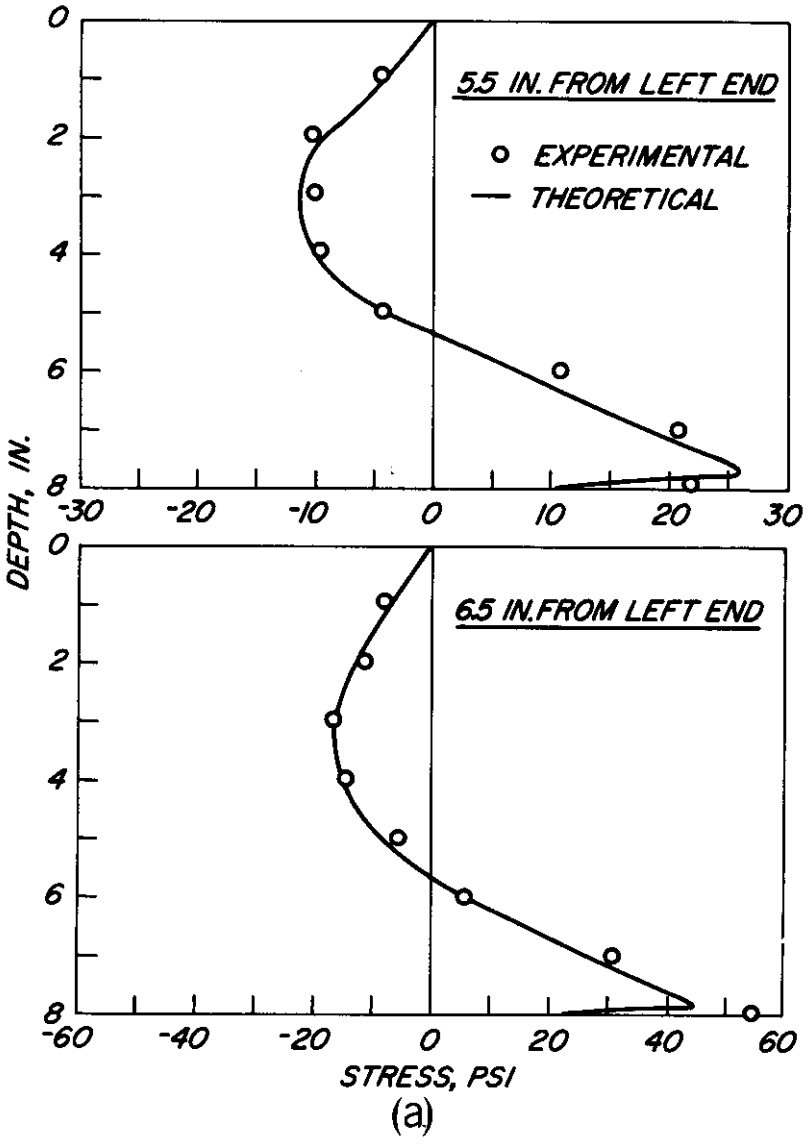

Figure 3.--Variations of shear stress vs. depth from top of simple beam (1 in. = 25.4 mm; 1 psi = 6.8947 x 10^3 N/m^2).

(M 146 768, 146 769, 146 770, 146 771)

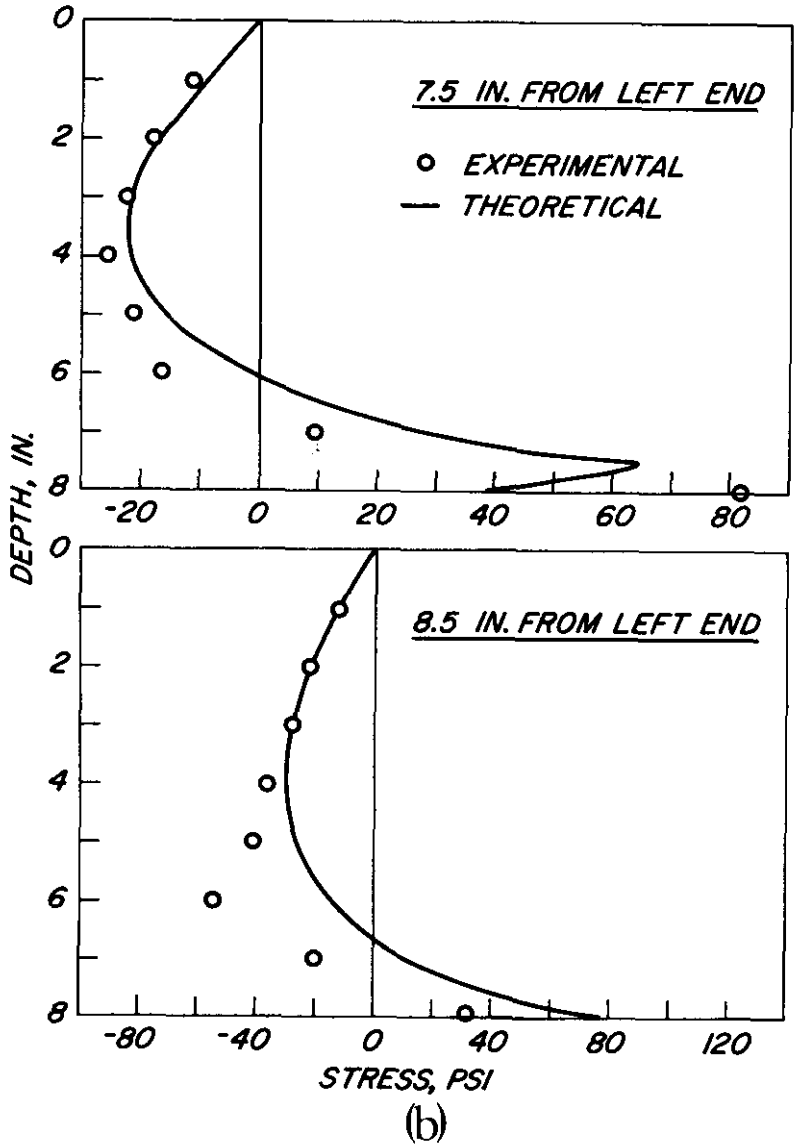

Figure 3.--Variations of shear stress vs. depth from top of simple beam (1 in. = 25.4 mm; 1 psi = 6.8947 x 10^3 N/m^2). (Continued)

(M 146 768, 146 769, 146 770, 146 771)

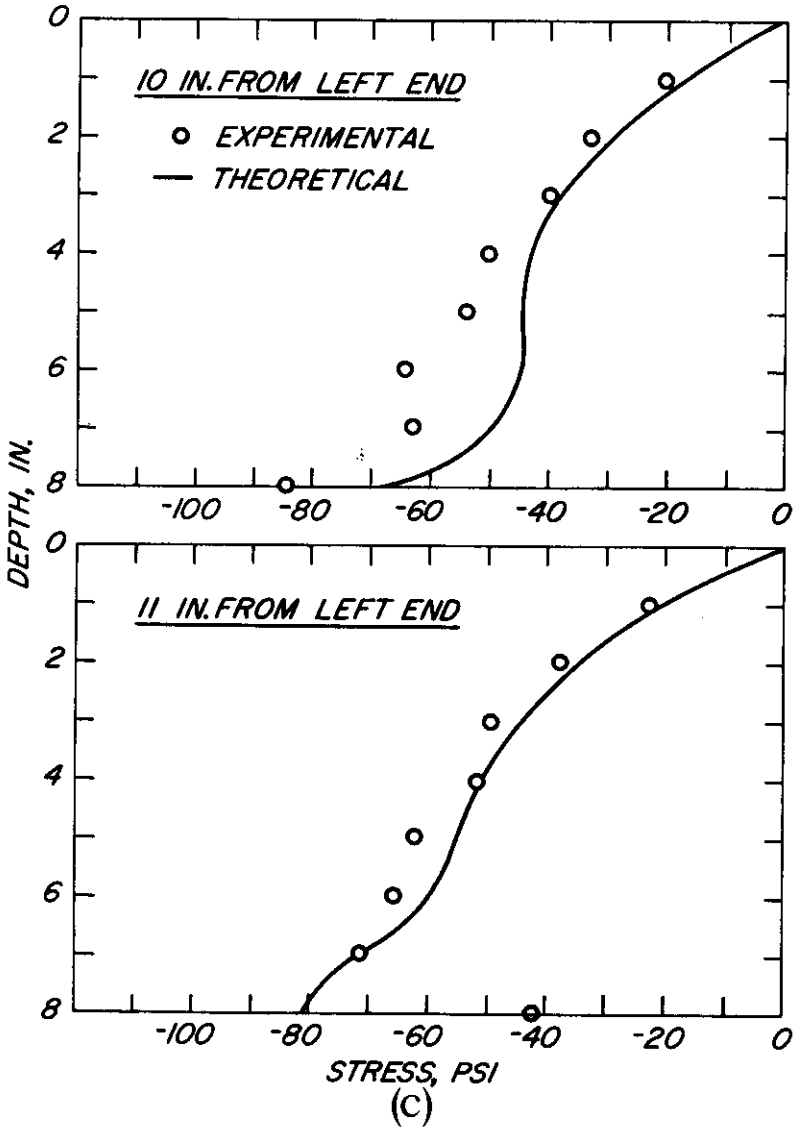

Figure 3.--Variations of shear stress vs. depth from top of simple beam (1 in. = 25.4 mm; 1 psi = 6.8947 x 10^3 N/m^2). (Continued)

(M 146 768, 146 769, 146 770, 146 771)

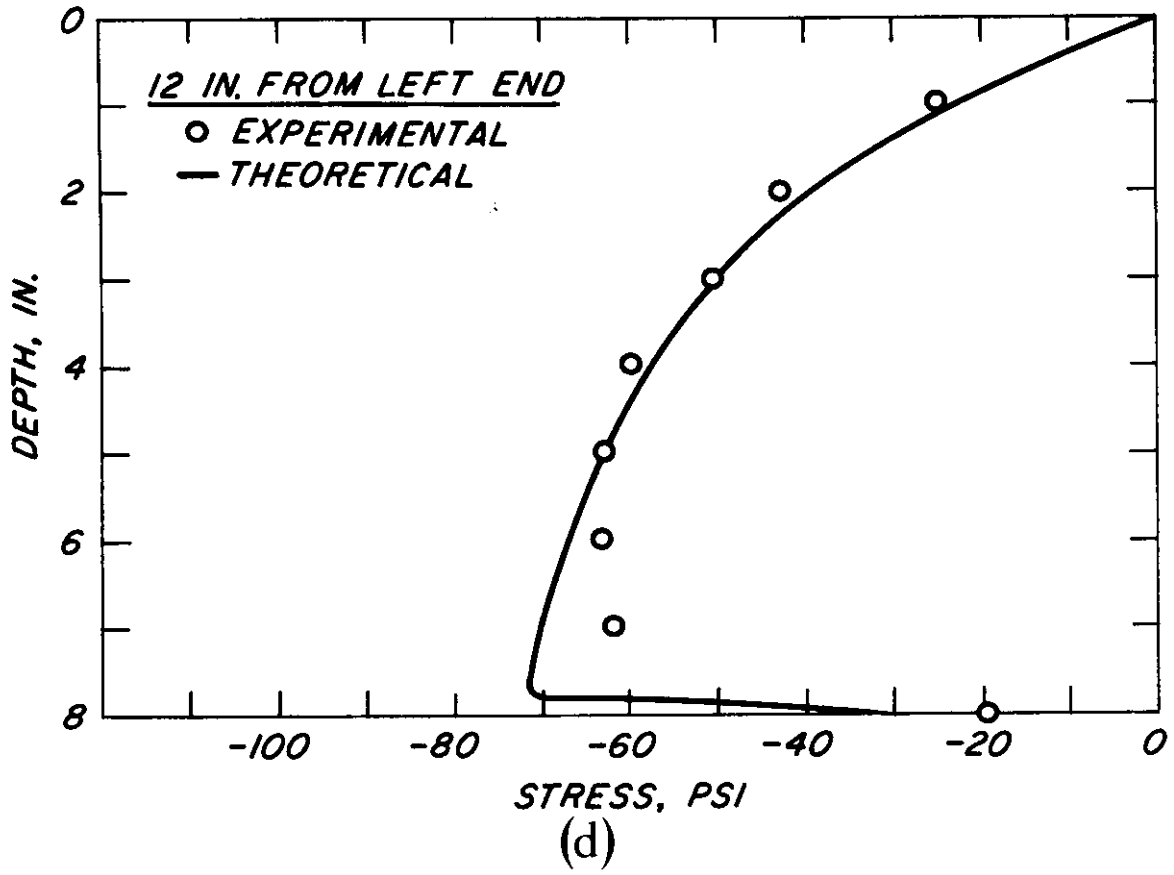

Figure 3.--Variations of shear stress vs. depth from top of simple beam (1 in. = 25.4 mm; 1 psi = 6.8947 x 10^3 N/m^2). (Continued)

(M 146 768, 146 769, 146 770, 146 771)

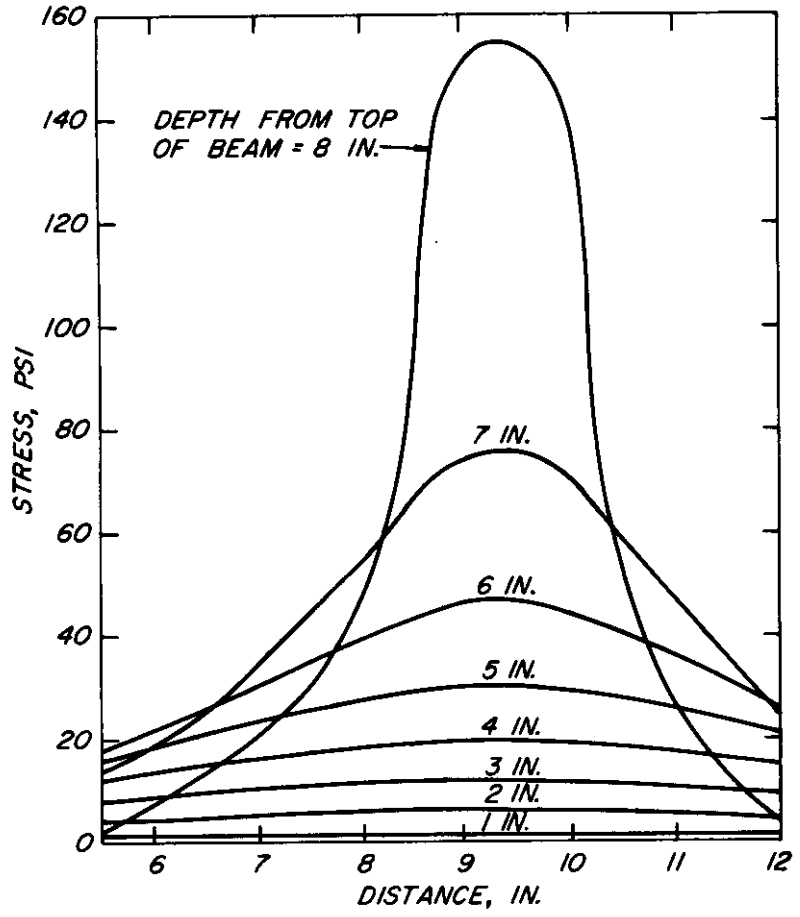

Figure 4.--Theoretical predictions of vertical compressive stress vs. distance from left end of simple beam; at left end of support x = 4.46 inches; at right end of support x = 10.46 inches. (1 in. = 25.4 mm; 1 psi = 6.8947 x 10^3 N/m^2).

(M 146 772)

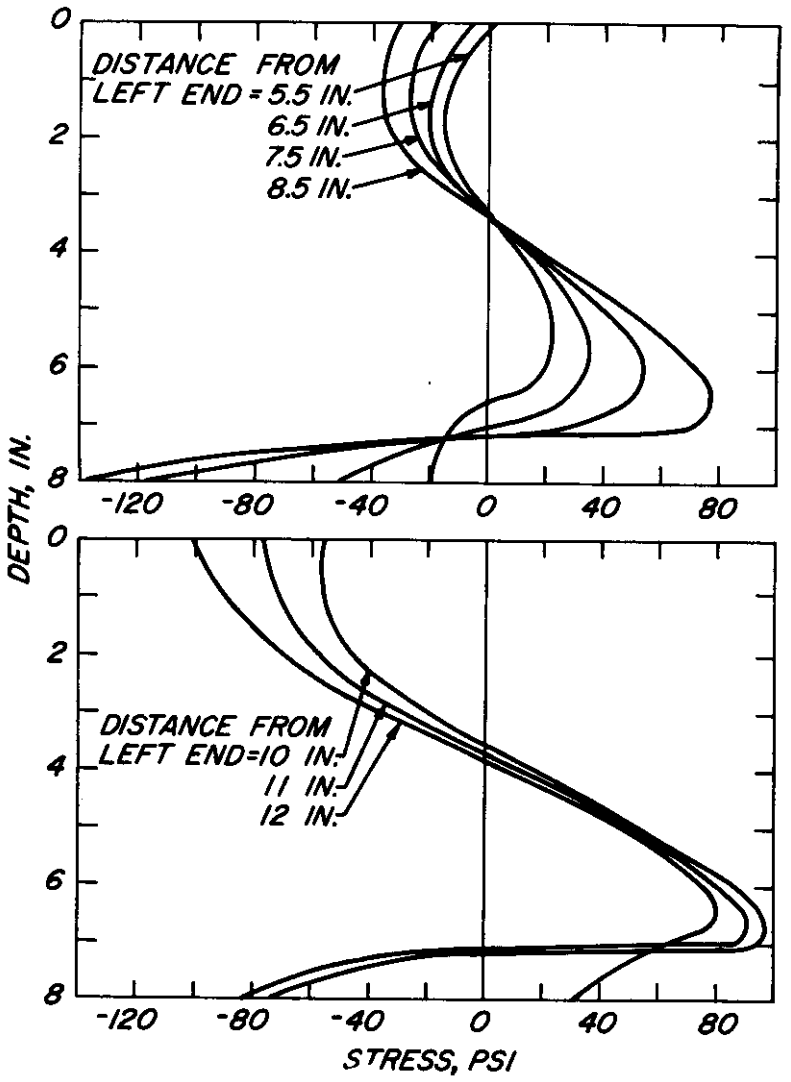

Figure 5.--Theoretical predictions of bending stress vs. depth from top of simple beam (1 in. = 25.4 mm; 1 psi = 6.8947 x 10^3 N/m^2).

(M 146 773)

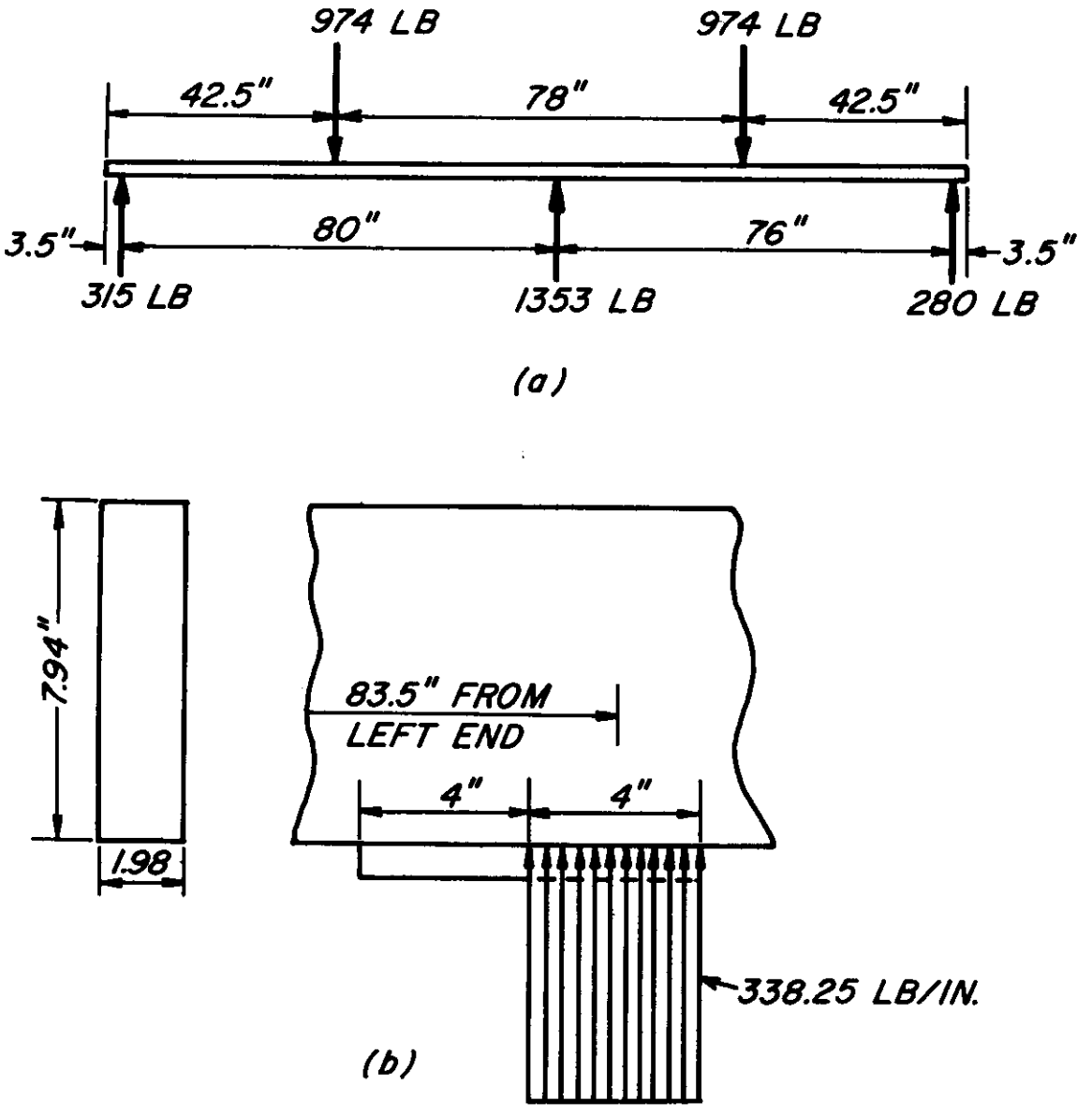

Figure 6.--Continuous beam (a) applied loads and reactions;
(b) assumed compressive forces at middle support
(1 in. = 25.4 mm; 1 lb. = 4.4482 N; 1 lb./in. = 175 N/m).
(M 146 774)

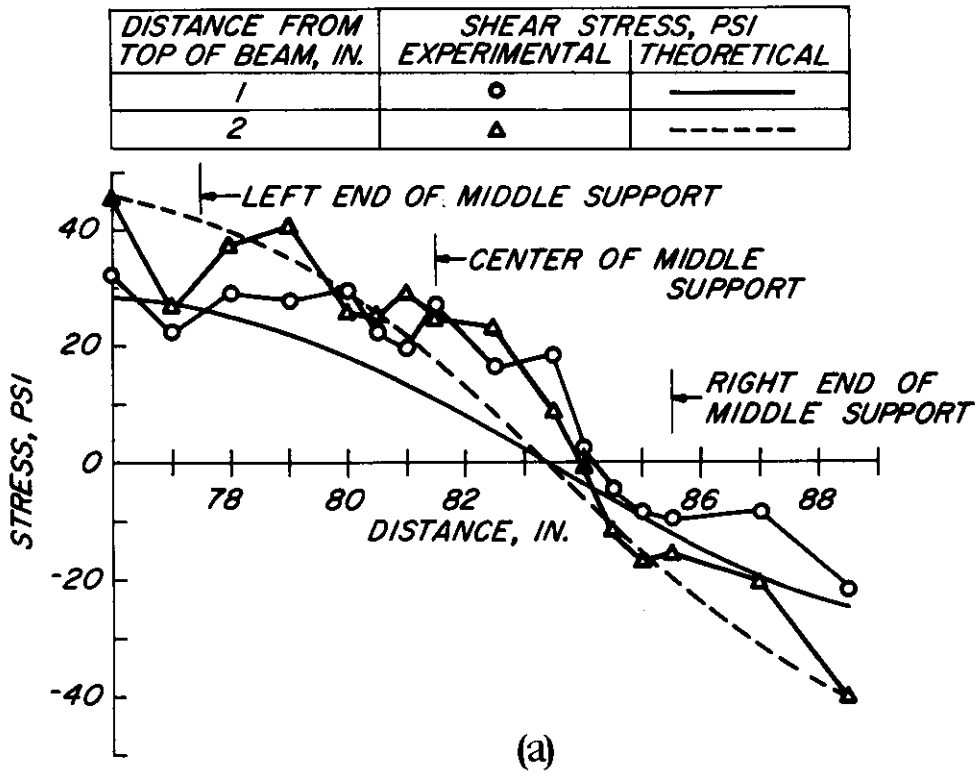

Figure 7.--Variations of shear stress vs. distance from left end of continuous beam (1 in. = 25.4 mm; 1 psi = 6.8947 x 10^3 N/m^2).

(M 146 775, 146 776, 146 777, 146 778)

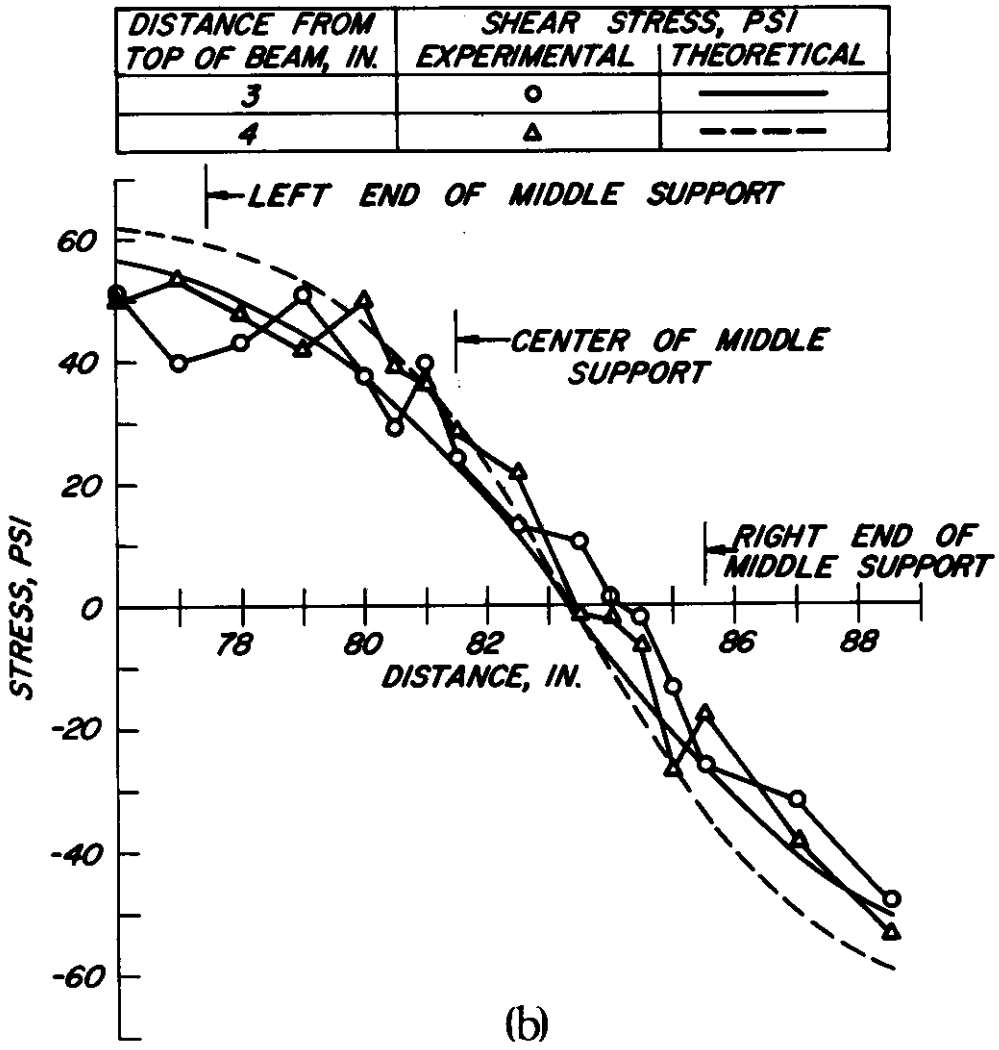

Figure 7.--Variations of shear stress vs. distance from left end of continuous beam (1 in. = 25.4 mm; 1 psi = 6.8947 x 10^3 N/m^2). (Continued)

(M 146 775, 146 776, 146 777, 146 778)

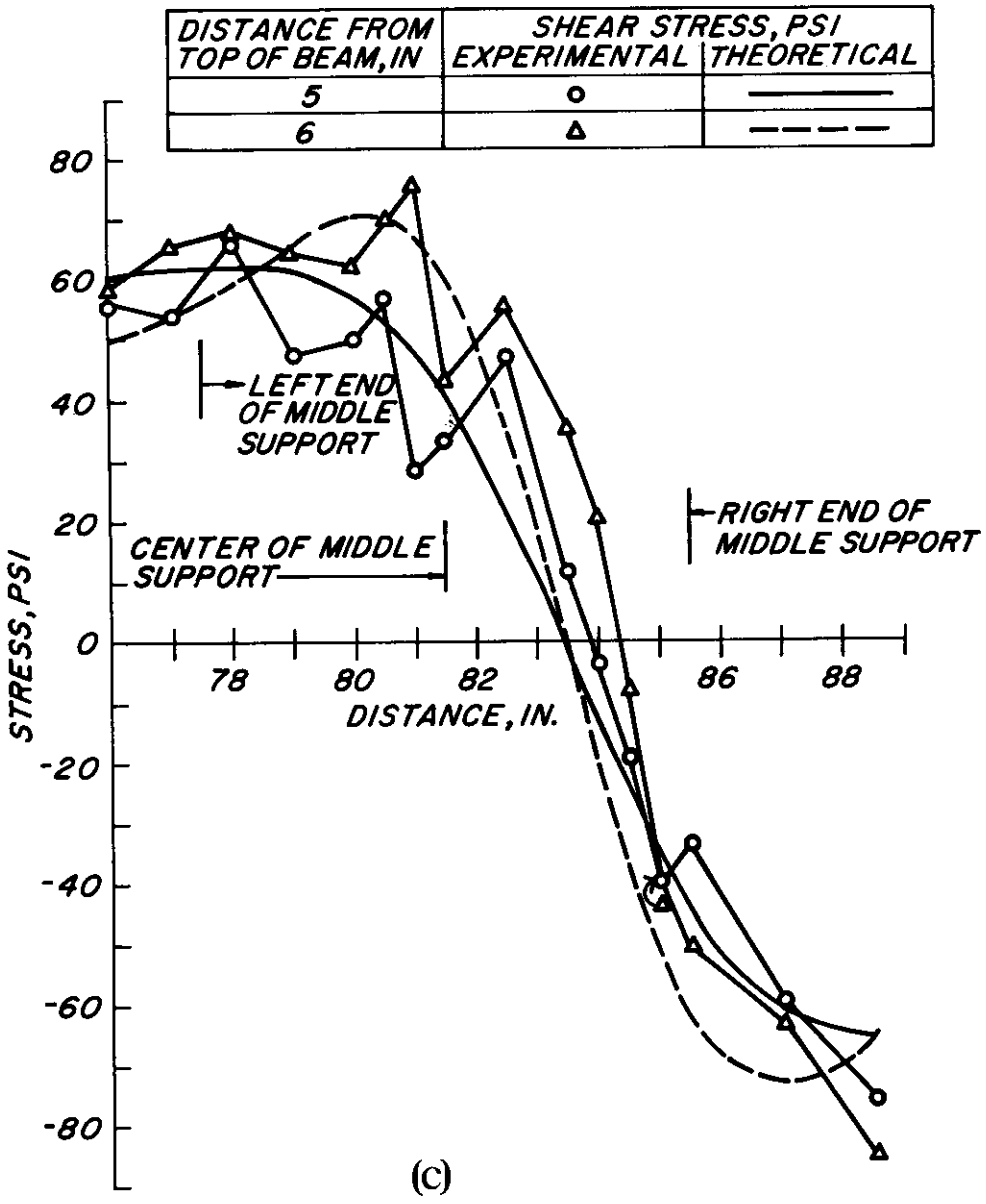

Figure 7.--Variations of shear stress vs. distance from left end of continuous beam (1 in. = 25.4 mm; 1 psi = 6.8947 x 10^3 N/m^2). Continued)

(M 146 775, 146 776, 146 777, 146 778)

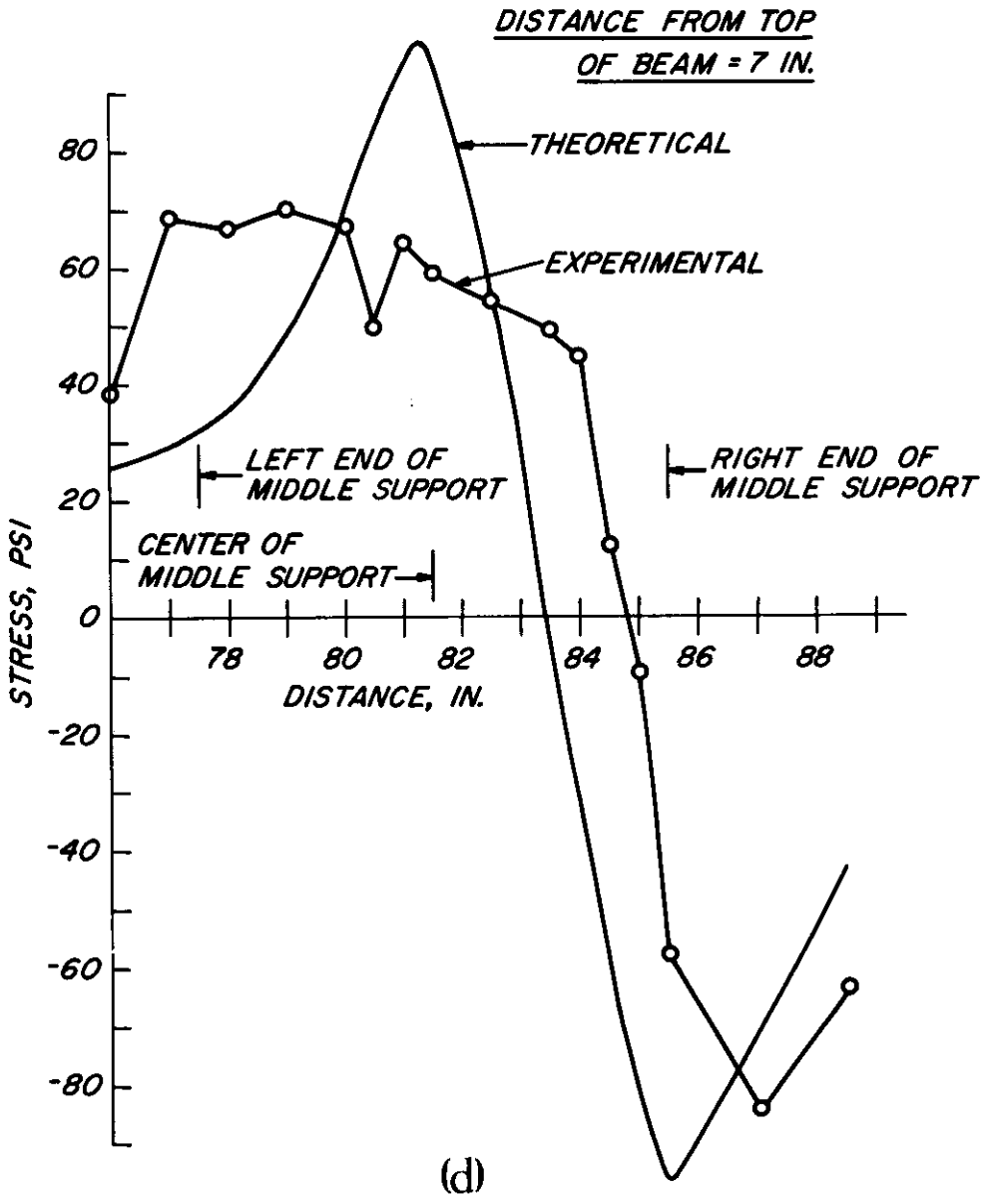

Figure 7.--Variations of shear stress vs. distance from left end of continuous beam (1 in. = 25.4 mm; 1 psi = 6.8947 x 10^3 N/m^2). (Continued)

(M 146 775, 146 776, 146 777, 146 778)

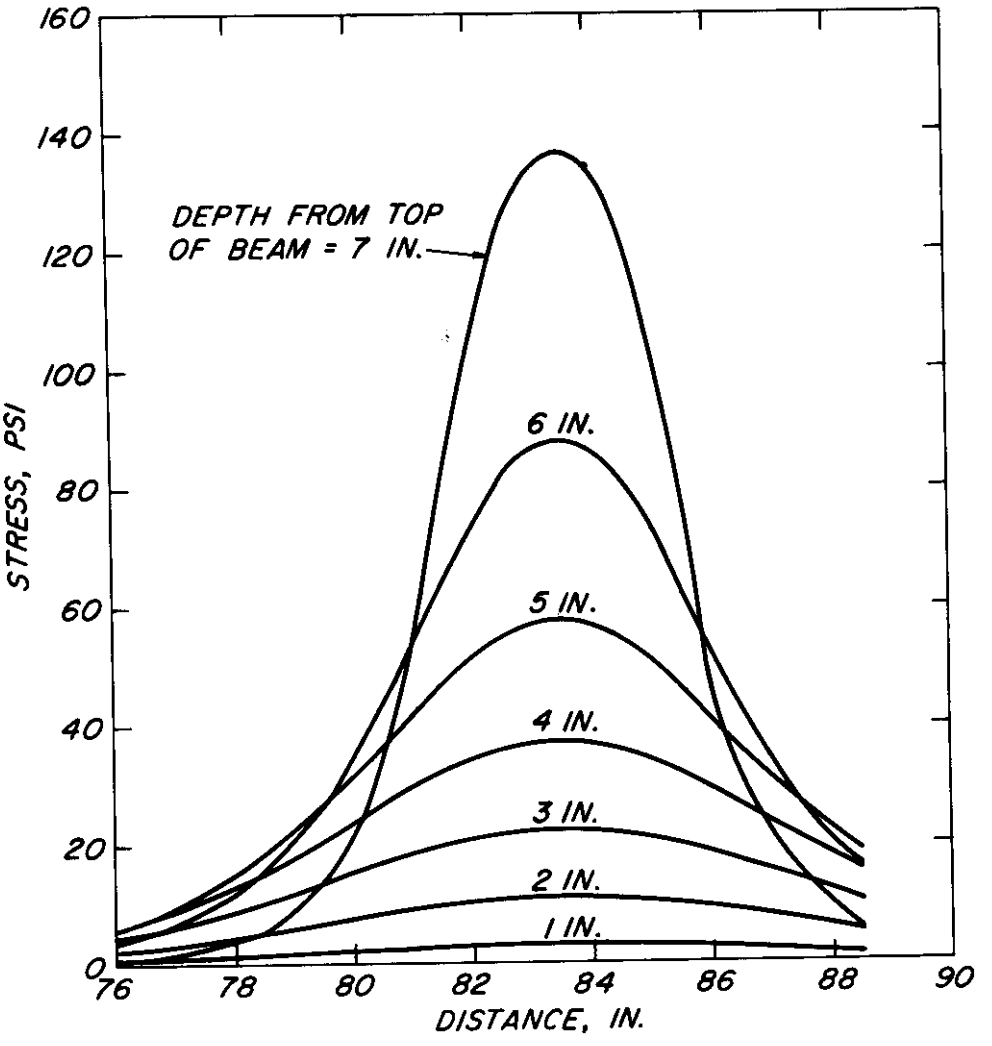

Figure 8.--Theoretical predictions of vertical compressive stress vs. distance from left end of continuous beam; at left end of middle support x = 77.5 in.; at right end of middle support x = 85.5 in. (1 in. = 25.4 mm; 1 psi = 6.8947 x 10^3 N/m^2).

(M 146 779)

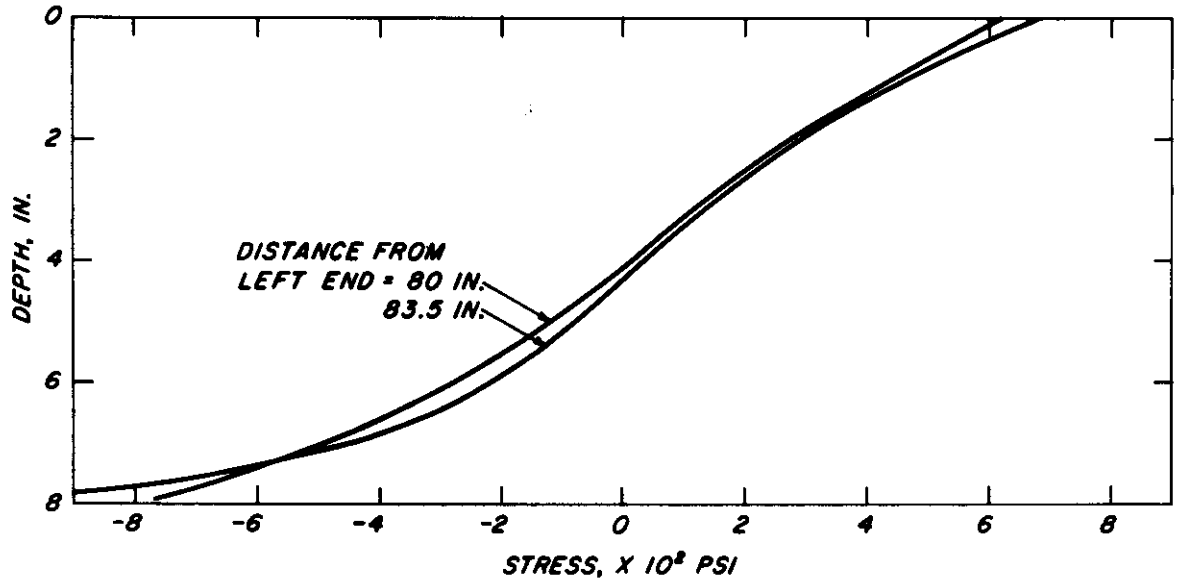

Figure 9.--Theoretical predictions of bending stress vs. depth from top of continuous beam (1 in. = 25.4 mm; 1 psi = 6.8947 x 10^3 N/m^2).

(M 146 780)

APPENDIX I.--FORMULATION OF ISOTROPIC BEAM

For an isotropic beam, one cannot obtain a solution by simply setting $\alpha = \beta = \varepsilon = 1$ in equations 13 and then substitute them into equations 5, 6, and 7, since this will cause the constants A_n, B_n, C_n, and D_n in these equations to become indeterminate. To effect the conversion, one must set $\varepsilon = 1$, $\beta = \frac{1}{\alpha}$ and then differentiate D, D_a, D_b, D_c, and D_d in equations 13 with respect to α twice before setting $\alpha = 1$. After some tedious algebraic manipulations, the following results are obtained:

$$\sigma_x = \sum_{n=1}^{\infty} \frac{m^2}{D''}[D_1\cosh my + D_2(2\cosh my + my\sinh my) + D_3\sinh my + D_4(2\sinh my + my\cosh my)]\sin mx \qquad \text{(I-1)}$$

$$\sigma_y = -\sum_{n=1}^{\infty} \frac{m^2}{D''}[D_1\cosh my + D_2 my\sinh my + D_3\sinh my + D_4 my\cosh my]\sin mx \qquad \text{(I-2)}$$

$$\tau = -\sum_{n=1}^{\infty} \frac{m^2}{D''}[D_1\sinh my + D_2(\sinh my + my\cosh my) + D_3\cosh my + D_4(\cosh my + my\sinh my)]\cos mx \qquad \text{(I-3)}$$

where

$$D'' = 4m^2(8m^2h^2 - \cosh 4mh + 1) \qquad \text{(I-4)}$$

$$D_1 = 4a_n[\cosh 3mh + mh\sinh 3mh$$

$$- (4m^2h^2+1)\cosh mh - 3mh\sinh mh] \qquad (I-5)$$

$$D_2 = 4a_n[4mh\sinh mh + \cosh mh$$

$$- \cosh 3mh] \qquad (I-6)$$

$$D_3 = 4a_n[mh\cosh 3mh + \sinh 3mh$$

$$+ (4m^2h^2 +1)\sinh mh + 3mh\cosh mh] \qquad (I-7)$$

$$D_4 = -4a_n[4mh\cosh mh + \sinh mh + \sinh 3mh] \qquad (I-8)$$

in which a_n is expressed by equation 8c.

It is to be noted that if the stress function for the isotropic case as described in reference (13) were used, one would have obtained the same results for the same loading condition as shown in figure lb. This also serves to confirm that the derivations for the orthotropic beam in the present study are correct.

The vertical deflection of the center line of the isotropic beam can be shown to take the following form:

$$Ev = \sum_{n=1}^{\infty} [-(1+\nu)\frac{mD_3}{D''} + (1-\nu)\frac{mD_4}{D''}]\cdot\sin mx$$

$$- EK_o x + K_2 \qquad (I-9)$$

which corresponds to equation 20 for the orthotropic beam.

APPENDIX II.--SIMPLIFIED FORMS OF STRESS COMPONENTS

It is possible to reduce the infinite series for each stress component to the sum of a finite series and a closed form. To do this, one can first express the hyperbolic functions in terms of exponential functions and then, after some simplifications, reduce the infinite series comprising exponential functions and trigonometrical functions to closed form.

A. ORTHOTROPIC BEAM

It can be shown that equation 13 can be reduced to

$$A_n = \frac{a_n}{m^2} \cdot \frac{\beta^2 - 1}{2-(\alpha^2+\beta^2)} \cdot e^{-m\varepsilon h\alpha} \tag{II-1}$$

$$B_n = \frac{a_n}{m^2} \cdot \frac{\alpha^2 - 1}{2-(\alpha^2+\beta^2)} \cdot e^{-m\varepsilon h\beta} \tag{II-2}$$

$$C_n = A_n \tag{II-3}$$

$$D_n = B_n \tag{II-4}$$

when $e^{-2m\varepsilon h\beta}$ is negligibly small compared with unity. Equations 5, 6, and 7 can now be expressed in the following form when a_n in equation 8c is used:

$$\sigma_x = \frac{2\varepsilon^2 P}{\ell[2-(\alpha^2+\beta^2)]} \cdot \sum_{n=1}^{\infty} [\alpha^2(\beta^2-1) \cdot e^{-m\alpha(\varepsilon h-\eta)} + \beta^2(\alpha^2-1) \cdot e^{-m\beta(\varepsilon h-\eta)}] \cdot [\cos m(a-x) - \cos m(a+x)] \tag{II-5}$$

$$\sigma_y = \frac{-P}{\ell[2-(\alpha^2+\beta^2)]} \cdot \sum_{n=1}^{\infty} [(\beta^2-1)e^{-m\alpha(\varepsilon h-\eta)} + (\alpha^2-1)e^{-m\beta(\varepsilon h-\eta)}] \cdot [\cos m(a-x) - \cos m(a+x)] \quad \text{(II-6)}$$

$$\tau = \frac{-\varepsilon P}{\ell[2-(\alpha^2+\beta^2)]} \cdot \sum_{n=1}^{\infty} [\alpha(\beta^2-1)e^{-m\alpha(\varepsilon h-\eta)} + \beta(\alpha^2-1)e^{-m\beta(\varepsilon h-\eta)}] \cdot [\sin m(a-x) + \sin m(a+x)] \quad \text{(II-7)}$$

For other expressions of a_η, the above equations need to be modified but the procedures of derivation remain the same.

From reference (6), the following identities can be derived:

$$\sum_{n=1}^{\infty} e^{-nq\theta} \cos n\theta = T_1 + T_2 \quad \text{(II-8)}$$

$$\sum_{n=1}^{\infty} e^{-nq\theta} \sin n\theta = -qT_1 + \frac{T_2}{q} \quad \text{(II-9)}$$

where

$$T_1 = \frac{1}{(1+q^2)} \left[\frac{e^{q\theta}(\cos\theta - q\sin\theta) - 1}{e^{q\theta}(e^{q\theta} - 2\cos\theta) + 1}\right], q>0$$

$$T_2 = \frac{qe^{-q\theta}}{(1+q^2)} \left[\frac{q\cos\theta + \sin\theta - q}{e^{-q\theta}(e^{-q\theta} - 2\cos\theta) + 1}\right], q>0$$

It can be seen that the series in equations II-5, II-6, and II-7 take the same form as either equation II-8 or equation II-9. Therefore, the stress components can all be reduced to closed form, which, thoughcomplicated, can easily be programed for a computer.

It is to be noted that the first terms in equations 5, 6, and 7 must be retained until n is so large that $e^{-2m\varepsilon h\beta}$ becomes negligibly small when compared with unity, and that the same number of terms must be deducted from equations II-5, II-6, and II-7 before the closed form expressions are added to the finite series. All these can easily be handled in a computer program.

B. ISOTROPIC BEAM

For the isotropic beam discussed in Appendix I, the following results are obtained:

$$\frac{m^2 D_1}{D''} = -a_n(mh + 1)e^{-mh} \tag{II-10}$$

$$\frac{m^2 D_2}{D''} = a_n e^{-mh} \tag{II-11}$$

$$D_3 = D_1 \tag{II-12}$$

$$D_4 = D_2 \tag{II-13}$$

when e^{-2mh} is small compared with unity. Again, with a_n represented by equation 8c, the stress components can be written as

$$\sigma_x = -\frac{P}{\ell} \sum_{n=1}^{\infty} [m(h-y)-1]e^{-m(h-y)} \cdot [\cos m(a-x) - \cos m(a+x)] \tag{II-14}$$

$$\sigma_y = \frac{P}{\ell} \sum_{n=1}^{\infty} [m(h-y)+1]e^{-m(h-y)}$$

$$\cdot \ [\cos m(a-x) - \cos m(a+x)] \qquad \text{(II-15)}$$

$$\tau = \frac{P}{\ell} \sum_{n=1}^{\infty} m(h-y)e^{-m(h-y)}$$

$$\cdot[\sin m(a-x) + \sin m(a+x)] \qquad \text{(II-16)}$$

To reduce the infinite series in these equations to closed form, in addition to equations II-8 and II-9, the following identities, also derived from (6), will be needed:

$$\sum_{n=1}^{\infty} ne^{-nq\theta}\cos n\theta = (1-q^2)T_3 + 2qT_4 \qquad \text{(II-17)}$$

$$\sum_{n=1}^{\infty} ne^{-nq\theta}\sin n\theta = -2qT_3 + (1-q^2)T_4 \qquad \text{(II-18)}$$

where

$$T_3 = e^{-q\theta} \{ \ (e^{-2q\theta}-1)[q^2(\cos\theta-1) + \cos\theta] + 2e^{-q\theta}(q\sin\theta-1)$$

$$+ 2 (\cos\theta - q\sin\theta)\} \ / \ [(1+q^2)(e^{-2q\theta}-2e^{-q\theta}\cos\theta + 1)]^2, \ q>0$$

$$T_4 = e^{q\theta} \ \{ (e^{2q\theta}-1)[(1-q^2)\sin\theta + 2q\cos\theta] + 4q(\cos\theta$$

$$- e^{q\theta})\} \ /[(1+q^2)(e^{2q\theta} - 2e^{q\theta}\cos\theta + 1)]^2, \ q>0$$

The numerical procedures are the same as in the orthotropic case.

APPENDIX III.--NOTATION

The following symbols are used in this paper:

A_n, B_n, C_n, D_n = constants of integration;

a = x-coordinate of a load point;

a_n = Fourier coefficients;

E_x, E_y = moduli of elasticity in x- and y-directions, respectively;

$f(h)$, $r(y)$, $s(x)$ = functions;

G_{xy} = modulus of rigidity associated with xy-plane;

h = half depth of beam;

$$K = \sqrt{\frac{E_x E_y}{2}} \left(\frac{1}{G_{xy}} - \frac{2\nu_{xy}}{E_x} \right)$$

K_o, K_1, K_2 = constants;

ℓ = length of beam;

$m = n\pi/\ell$;

n = integer;

P = applied load;

$p(x)$ = load function;

u, v = displacements in x-and y-directions, respectively;

x, y = Cartesian coordinates

$$\alpha = \sqrt{K + \sqrt{K^2 - 1}}$$

$$\beta = \sqrt{K - \sqrt{K^2 - 1}}$$

$$\varepsilon = \sqrt[4]{\frac{E_x}{E_y}}$$

$$\eta = \varepsilon y$$

ϕ = stress function;

ν_{xy} = Poisson's ratio associated with stress in x-direction and strains in x- and y-directions;

σ_x, σ_y = normal stresses in x- and y-directions, respectively;

τ = orthogonal shear stress.

REFERENCES

1. Boley, B. A., and I. S. Tolins.
   1956. On the stresses and deflections of rectangular beams, Journal of Applied Mechanics, ASME trans., Vol. 23, No. 3, p. 339-342, Sept.

2. Conway, H. D.
   1952. Bending of orthotropic beams, Journal of Applied Mechanics ASME trans, Vol. 19, No. 2, p. 227, June.

3. Conway, H. D.
   1953. Some problems of orthotropic plane stress, Journal of Applied Mechanics, ASME trans., Vol 20, No. 1, p. 72-76, Mar.

4. Cowan, W. C.
   1962. Shear stress in two wood beams over wood block supports, U.S. For. Prod. Lab., FPL Rep. No. 2249, Aug.

5. Donnell, L. H.
   1952. Bending of rectangular beams, Journal of Applied Mechanics, ASME trans., Vol. 19, No. 1, p. 123, Mar.

6. Edwards, J.
   1922. Treatise on integral calculus, Vol. II, Chelsea Publishing Co., New York.

7. Green, A. E.
   1939. Stress systems in aeolotropic plates, part 2, Proceedings, Royal Society of London, Vol. 173, p. 173-192.

8. Hashin, Z.
   1967. Plane anisotropic beams, Journal of Applied Mechanics, ASME trans., Vol. 34, No. 2, p. 257-262, June.

9. Hooley, R. F., and P. D. Hibbert.
   1967. Stress concentration in timber beams, Journal of Structural Division, Proceedings of ASCE, Vol. 93, No. ST2, p. 127-139, April.

10. Lamb, H.
    1909. Flexure of a narrow beam, Atti IV Cong. Intern. Matemat. (Rome), Vol. 3, p. 12-32.

11. Silverman, I. K.
1964. Orthotropic beams under polynomial loads, Journal of Engineering Mechanics Division, Proceedings of ASCE, Vol. 90, No. EM5, p. 293-319, Oct.

12. Smith, C. B. and A. W. Voss.
1948. Stress Distribution in a beam of orthotropic material subjected to a concentrated load, Nat. Adv. Comm. Aeron. Tech. Note 1486, Mar.

13. Timoshenko, S., and J. N. Goodier.
1951. Theory of Elasticity, second ed., McGraw-Hill Book Co., Inc.

GPO 822–805